International Journal of Nanomedicine

Dovepress
Taylor & Francis Group

Open Access Full Text Article

ORIGINAL RESEARCH

Exosomes Derived from Apelin-Pretreated Mesenchymal Stem Cells Ameliorate Sepsis-Induced Myocardial Dysfunction by Alleviating Cardiomyocyte Pyroptosis via Delivery of miR-34a-5p

Ting Li[1,2,*], Yuechu Zhao[3,*], Zhi Cao[2,*], Ying Shen[2], Jiaqi Chen[2], Xinran Huang[2], Zhuang Shao[2], Yi Zeng[2], Qi Chen[2], Xiaofei Yan[3], Xin Li[1,2], Yuelin Zhang[1,2], Bei Hu[1,2]

[1]School of Medicine, South China University of Technology, Guangzhou, Guangdong, People's Republic of China; [2]Department of Emergency Medicine, Guangdong Provincial People's Hospital (Guangdong Academy of Medical Sciences), Southern Medical University, Guangzhou, Guangdong, People's Republic of China; [3]Guangdong Cardiovascular Institute, Guangdong Provincial People's Hospital (Guangdong Academy of Medical Sciences), Southern Medical University, Guangzhou, Guangdong, People's Republic of China

*These authors contributed equally to this work

Correspondence: Yuelin Zhang; Bei Hu, Department of Emergency Medicine, Guangdong Provincial People's Hospital (Guangdong Academy of Medical Sciences), Southern Medical University, Guangzhou, Guangdong, 510080, People's Republic of China, Tel +86-20-83827812-20974, Email zhangyuelin1999@163.com; qhubei@hotmail.com

Background: Exosomes sourced from mesenchymal stem cells (MSC-EXOs) have become a promising therapeutic tool for sepsis-induced myocardial dysfunction (SMD). Our previous study demonstrated that Apelin pretreatment enhanced the therapeutic benefit of MSCs in myocardial infarction by improving their paracrine effects. This study aimed to determine whether EXOs sourced from Apelin-pretreated MSCs (Apelin-MSC-EXOs) would have potent cardioprotective effects against SMD and elucidate the underlying mechanisms.

Methods: MSC-EXOs and Apelin-MSC-EXOs were isolated and identified. Mice neonatal cardiomyocytes (NCMs) were treated with MSC-EXOs or Apelin-MSC-EXOs under lipopolysaccharide (LPS) condition in vitro. Cardiomyocyte pyroptosis was determined by TUNEL staining. RNA sequencing was used to identify differentially expressed functional miRNAs between MSC-EXOs and Apelin-MSC-EXOs. MSC-EXOs and Apelin-MSC-EXOs were transplanted into a mouse model of SMD induced by cecal ligation puncture (CLP) via the tail vein. Heart function was evaluated by echocardiography.

Results: Compared with MSC-EXOs, Apelin-MSC-EXO transplantation greatly enhanced cardiac function in SMD mice. Both MSC-EXOs and Apelin-MSC-EXOs suppressed cardiomyocyte pyroptosis in vivo and in vitro, with the latter exhibiting superior protective effects. miR-34a-5p effectively mediated Apelin-MSC-EXOs to exert their cardioprotective effects in SMD with high mobility group box-1 (HMGB1) as the potential target. Mechanistically, Apelin-MSC-EXOs delivered miR-34a-5p into injured cardiomyocytes, thereby ameliorating cardiomyocyte pyroptosis via regulation of the HMGB1/AMPK axis. These cardioprotective effects were partially abrogated by downregulation of miR-34a-5p in Apelin-MSC-EXOs.

Conclusion: Our study revealed miR-34a-5p as a key component of Apelin-MSC-EXOs that protected against SMD via mediation of the HMGB1/AMPK signaling pathway.

Keywords: Exosomes, mesenchymal stem cells, apelin, sepsis-induced myocardial dysfunction, pyroptosis

Introduction

Sepsis, a life-threatening systemic inflammatory disorder, is a major cause of mortality in hospital.[1–3] Septic myocardial dysfunction (SMD) is a widespread complication of sepsis and accounts for >40% of septic patients and a mortality rate

Received: 30 September 2024
Accepted: 5 January 2025
Published: 17 January 2025

Graphical Abstract

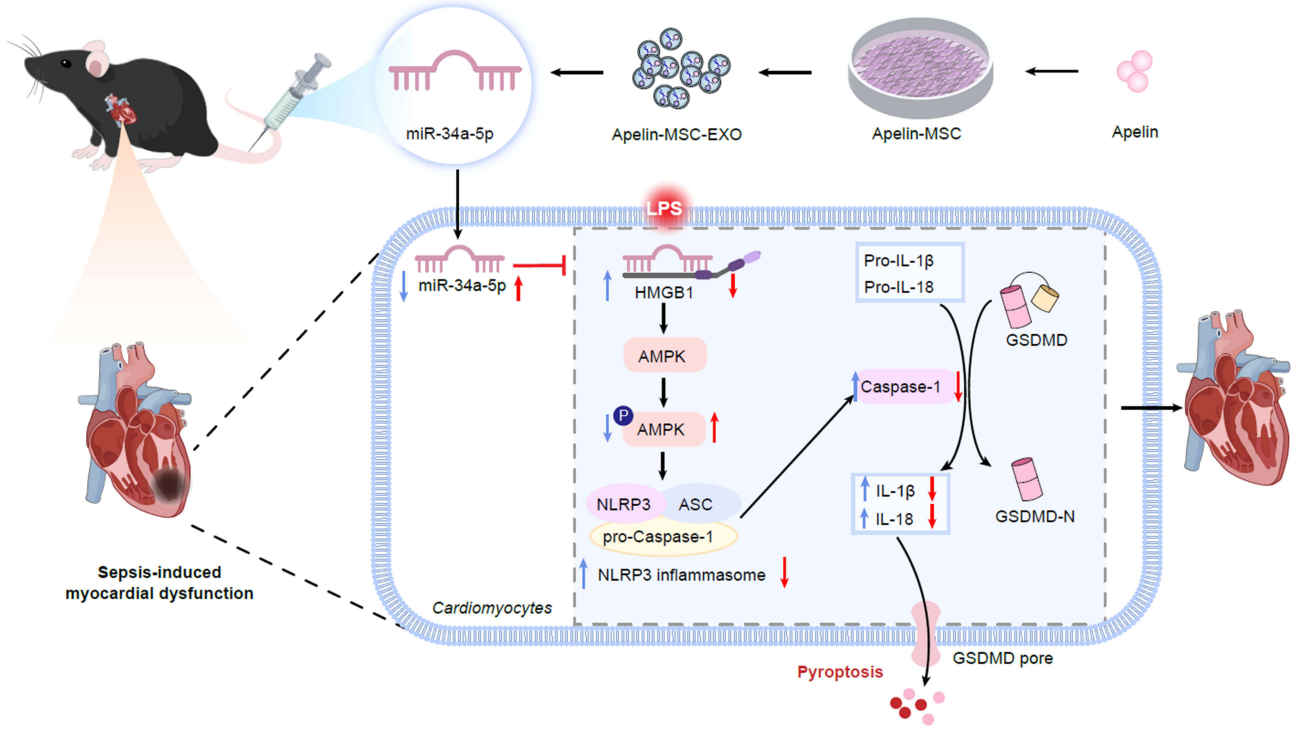

approaching 70% in sepsis.[4,5] Despite encouraging results from vasopressor drugs, beta blockers and mechanical assistance, clinical treatments for SMD remain limited, partially due to its extremely complex pathogenesis.[6,7] It is vital to understand the molecular mechanisms of SMD and develop more effective treatments.

Accumulating studies show that mesenchymal stem cell (MSC)-derived exosomes (EXOs), a key effector of MSC paracrine function, have great potential in SMD treatment.[8] MSC-derived exosomal circRTN4 has been shown to attenuate cardiac injury and apoptosis in a rat model of SMD model by mediating the miR-497-5p/MG53 axis.[9] Studies have shown that pretreatment with some pharmacologic compounds can increase the paracrine effects of MSCs including EXOs and then improve their therapeutic effects in cardiovascular diseases.[10,11] Apelin is an endogenous peptide that binds to the angiotensin-like 1 (APJ) receptor. Both the apelin and APJ genes are expressed in a wide range of tissues, with distribution patterns similar to those of the angiotensin II (Ang II) and AT1 receptors.[12] Research in animal models has indicated that the apelin-APJ system plays an important role in cardiovascular regulation.[13,14] Apelin is known to function as a potent inotropic agent and peripheral vasodilator, and may also contribute to fluid balance, making it a promising candidate for therapeutic strategies in heart failure.[15] More importantly, we demonstrated that Apelin pretreatment significantly augmented the cardioprotective effects of MSCs on myocardial injury following infarction by upregulating the paracrine effects.[16] Nonetheless the therapeutic efficacy of Apelin pretreated MSC-derived EXOs (Apelin-MSC-EXOs) on SMD have not been determined.

Although the complete mechanisms of SMD remain elusive, cardiomyocyte pyroptosis, a unique type of inflammatory cell death, is linked to the condition.[17–19] Pyroptosis is predominately triggered by Nod-like receptor protein 3 inflammasome (NLRP3) that is composed of NLRP3, apoptosis-associated speck-like protein (ASC) and procaspase-1.[20] NLRP3 inflammasome triggers the activation of inflammatory caspase-1 and then cleaves gasdermin D (GSDMD) to produce N-terminal GSDMD (GSDMD-NT), leading to pyroptosis and secretion of IL-18 and IL-1β.[21,22] Yang et al reported that TREM-1 induced cardiomyocyte pyroptosis in cecal ligation and puncture (CLP)-induced SMD in mice via

activation of the SMC4/NEMO pathway.[23] Therefore, inhibition of NLRP3 inflammasome-mediated cardiomyocyte pyroptosis offers possible strategy against SMD.

In the current study, we determined whether Apelin-MSC-EXOs exhibited a superior therapeutic efficacy in SMD treatment and illustrate the molecular mechanisms linked to cardiomyocyte pyroptosis.

Methods and Materials

Cell Culture

The MSCs derived from bone marrow and used in the current study were provided by Dr. Xiaoting Liang from Shanghai East Hospital. This study was approved by the research ethics board of Shanghai East Hospital (No. 2016–050). MSCs were cultured as previously described.[16] MSCs at passage 3~5 were used in this study. Neonatal mice cardiomyocytes (NMCs) were collected from 0- to 1-day-old mice as previously reported[24] and cultured on Claycomb Medium (51800, Sigma) containing 10% fetal bovine serum. All animal experiments were approved by Guangdong Provincial People's Hospital Ethics Committee (KY-Z-2020-363-02). The study was conducted in strict accordance with the Animal Management Rules of the Ministry of Health of the People's Republic of China.

MSC-EXO Isolation and Characterization

$1x10^6$ MSCs were seeded in a culture dish and cultured for 24h under normoxic conditions in complete medium with or without 0.1 nM Apelin-13 treatment as reported in our previous study.[16] Medium was then discarded and replaced by DMEM supplemented 10% exosome-free fetal bovine serum (EXO-FBS-250A-1, Systems Biosciences) and culture continued for 48h. Subsequently, the supernatant was collected and MSC-EXOs or Apelin-MSC-EXOs isolated and purified as previously reported.[25] The concentration of MSC-EXOs was measured. Particle size, surface markers and morphology of MSC-EXOs or Apelin-MSC-EXOs was examined by nanoparticle tracking analysis (NTA, PARTICLE METRIX-ZetaVIEW, Germany), Western blotting and transmission electron microscopy (TEM, Hitachi-HT7700, Tokyo, Japan), respectively. Specifically, 5μL of the extracted exosomes were added dropwise onto a copper grid and allowed to settle for 1 minute, after which the excess liquid was absorbed with filter paper. Then, 5μL of uranyl acetate was added dropwise onto the copper grid and allowed to settle for 1 minute, followed by absorption of the excess liquid with filter paper. The grid was air-dried for several minutes at room temperature. Transmission electron microscopy (TEM) imaging was performed at 100 kV to obtain TEM images. For exosome sample size analysis, frozen exosome samples were thawed in a 25°C water bath, placed on ice, diluted with 1 × PBS, and subjected to nanoparticle tracking analysis (NTA).

MSC-EXO Internalization

MSC-EXOs or Apelin-MSC-EXOs were labelled using PKH67 (MINI67-1KT, Sigma) and then cultured for 24h with NMCs in the presence of 1μg/mL LPS (L4391, Sigma). Next, after staining with DAPI, NMCs were randomly photographed under fluorescence microscopy.

TUNEL Staining

Pyroptosis of NMCs were evaluated using a TUNEL staining kit (RIBOBIO, C11026-1). NMCs were plated in twenty-four-well plates and then treated with 10μg/mL MSC-EXOs or Apelin-MSC-EXOs in 1μg/mL LPS for 24h. Next, the cells were stained with the TUNEL kit. Next, NMCs were stained with DAPI and captured. The pyroptosis rate was analyzed by the ratio of TUNEL positive NMCs to the total number of NMCs×100%.

MiR-34a-5p Inhibitor or Transfection

MiR-Control, miR-34a-5p inhibitor and miR-34a-5p mimic were obtained from GenePharma (Shanghai, China). NMCs were seeded on the culture plate and incubated for 24h. Next, NMCs were treated with 50 nM miR-Control, miR-34a-5p inhibitor or miR-34a-5p mimic by Lipofectamine 2000 (11668027, Invitrogen) and then cultured for 48h. Finally, the

transfection efficiency was evaluated by qRT-PCR. For miR-34a-5p^{KD}-Apelin-MSC-EXO isolation, MSCs were cultured under Apelin and transfected with miR-34a-5p inhibitor for 48h and EXOs isolated accordingly.

Luciferase Activity Assay

The 3′-UTR of wild-type HMGB1 or mutant HMGB1 luciferase reporter vector was established as previously reported.[26] 293T cells were co-transfected with miR-Control, miR-34a-5p mimic or inhibitor and the reporter plasmid using Lipofectamine 2000 for 48h. Luciferase activity was assessed by a Dual-Luciferase Reporter Assay Kit (E1910, Promega).

Real-Time PCR

Total RNA from MSC-EXOs, Apelin-MSC-EXOs or MSCs was collected by TRIzol reagent (2270A, Takara). Reverse transcription was carried out according to the protocol (RR037A, Takara). RT-PCR of miR-34a-5p and HMGB1 was determined using a quantitative PCR kit (RR820A, Takara). The U6 and miR-34a-5p primers were purchased from GenePharma.

MiRNA Sequencing and Analysis

The miRNA from Apelin-MSC-EXOs and MSC-EXOs was sequenced as previously described.[26] After normalizing the raw reads, the level of miRNAs was analyzed to discover significant differences between Apelin-MSC-EXO and MSC-EXO data sets. The different expression of miRNAs was analyzed through Q value < 0.001 and fold change > 1.5 with the threshold set for down- and up-regulated genes. Heat maps of different expression of miRNAs from MSC-EXOs and Apelin-MSC-EXOs were created using the omicshare cloud platform.

Western Blotting

NMCs and Heart tissue from different groups were collected and total protein extracted. The protein concentration of different samples was measured by BCA kit (231227, Thermo). A total of 30μg protein was separated on SDS-PAGE gel and then transferred onto PVDF membranes. Next, PVDF membranes were blocked with TBST supplemented with 5% fat-free milk and incubated at 4°C overnight with the relevant primary antibodies: anti-CD63 (ab134045, Abcam), anti-CD81 (ab109201, Abcam), anti-Alix (ab186429, Abcam), anti-TSG101 (ab125011, Abcam), anti-NLRP3 (ab263899, Abcam), anti-ASC (A1170, ABclonal), anti-Pro Caspase-1 (ab179515, Abcam), anti-Caspase-1 (A0964, ABclonal), anti-IL-18 (A1115, ABclonal), anti-IL-1β (26,048-1-AP, Proteintech), anti-GSDMD (ab209845, Abcam), anti-GSDMD-NT (AF4012, Affinity), anti-HMGB1 (ab18256, Abcam), anti-AMPK (ab32047, Abcam), anti-p-AMPK (AF3423, Affinity) and GAPDH (ab8245, Abcam). After washing with TBST, PVDF membranes were incubated with the secondary antibody for 1h at room temperature. Subsequently, PVDF membranes were exposed to radiography film in a dark room. Finally, the protein bands were analyzed by Image J software.

Animal Study

All animal experiments were conducted in accordance with the ARRIVE 2.0 guidelines and approved by Guangdong Provincial People's Hospital Ethics Committee (KY-Z-2020-363-02). The study was conducted in strict accordance with the Animal Management Rules of the Ministry of Health of the People's Republic of China. All experimental mice were housed under specific pathogen-free (SPF) conditions, with ambient temperature maintained at 22±2°C, relative humidity at 50±10%, and a 12-hour light/dark cycle. Mice had ad libitum access to standard chow and water, and the housing environment complied with the relevant requirements of the animal ethics committee. The SMD model was established in 6~8 week old C57BL/6 male mice by CLP as previously reported.[27] After anesthetizing the mice with 2% isoflurane, they were placed in a supine position supine on a sterile operating surface. The abdominal fur was shaved, and the skin disinfected with iodine. A 1 cm longitudinal incision was made along the midline, and the cecum gently manipulated using smooth forceps. For the moderate sepsis model, 60% of the cecum was ligated with surgical sutures, and two punctures made at the midpoint of the caudal end of the ligated cecum using an 18-gauge needle. Following manual extrusion of part of the intestinal content, the cecum was repositioned in the abdominal cavity, and the abdominal layers

closed with a 3–0 surgical suture. After the procedure, the mice were resuscitated with a subcutaneous injection of 0.9% sodium chloride solution (1 mL/20 g) into the abdomen and placed on warm blankets until they regained consciousness and were returned to their cages. In the sham group, mice received the surgery without cecum ligation and puncture (n=6). One dose of MSC-EXOs, Apelin-MSC-EXOs or miR-34a-5p^{KD}-Apelin-MSC-EXOs (2μg/g per mouse) in 100μL PBS was injected into SMD mice at 1h following CLP (n=10) via the tail vein.[28,29] Cardiac function of mice with different treatments was examined 24h following CLP surgery using transthoracic echocardiography (Ultramark 9). The left ventricular internal diameter during systole or diastole (LVIDs, LVIDd), left ventricle fractional shortening (LVFS) and ejection fraction (LVEF) were analyzed. Mice were euthanized 24 hours after the procedure, following cardiac ultrasound, and serum and heart tissue collected for subsequent experiments.

HE Staining

The mice from different groups were sacrificed by cervical dislocation under anesthesia. Heart tissue was collected, embedded and sectioned into 5μm slices. Next, hematoxylin eosin staining was performed following the protocol. Finally, myocardial tissue structures were captured under a microscope.

Statistical Analysis

All data are represented as mean±SEM. Statistical analyses were determined by GraphPad Prism 9.3.0. The results from two groups (=2) were analyzed using a *T* test. For comparisons of data from multiple groups (≥ 3), one-way analysis of variance (ANOVA) followed by the Bonferroni test was performed. $P\ value < 0.05$ was considered statistically significant.

Results

Apelin-MSC-EXOs and MSC-EXOs Characterization

Apelin-MSC-EXOs and MSC-EXOs were extracted from Apelin pretreated MSCs and MSCs at passage 3~5, respectively. TEM demonstrated that both Apelin-MSC-EXOs and MSC-EXOs displayed a spheroid morphology (Figure 1A). The NTA results revealed that most MSC-EXOs and Apelin-MSC-EXOs exhibited a distribution between 30 and 150 nm (Figure 1B). Importantly, the concentration of nanoparticles was much higher in Apelin-MSC-EXOs than MSC-EXOs (Figure 1B). The exosomal typical markers CD81, TSG101, CD63 and Alix were positive in MSC-EXOs and Apelin-MSC-EXOs (Figure 1C). Furthermore, the Apelin level in Apelin-MSC-EXOs was higher than that in MSC-EXOs (Figure 1C). Next, NMCs were incubated with PKH67-labelled MSC-EXOs and Apelin-MSC-EXOs under LPS condition for 24h. Confocal images showed that PKH67-labelled MSC-EXOs and Apelin-MSC-EXOs were endocytosed by NMCs (Figure 1D). These results showed that MSC-EXOs and Apelin-MSC-EXOs were successfully collected and taken up by NMCs under LPS challenge.

Apelin-MSC-EXO Transplantation Improved Heart Function in a Mouse Model of SMD

To evaluate the protective effects of Apelin-MSC-EXOs on SMD, one dose of MSC-EXOs or Apelin-MSC-EXOs was delivered into mice with SMD induced by CLP via the tail vein at 1h following CLP. The procedure for animal experiments is listed in Figure 2A. Representative echocardiographic images of the heart from different groups at 24h after CLP are shown in Figure 2B. As shown in Figure 2C, compared with the sham group, LVIDd and LVIDs were greatly enhanced in the CLP group but significantly decreased in the MSC-EXO and Apelin-MSC-EXO group, to a greater extent in the latter (Figure 2C). LVEF and LVFS were significantly reduced in the CLP group compared with the sham group (Figure 2C). Notably, compared with the CLP group, both LVEF and LVFS were increased in the MSC-EXOs group and Apelin-MSC-EXOs group, again to a greater extent in the latter (Figure 2C). Next, we examined the histopathological changes in mouse myocardial tissue from different groups. The results of HE staining revealed that compared with sham mice, apparent inflammatory infiltration and broken myocardial fibers in the myocardium were evident in CLP-treated mice. This phenomenon was partially reversed in the MSC-EXO group and Apelin-MSC-EXO

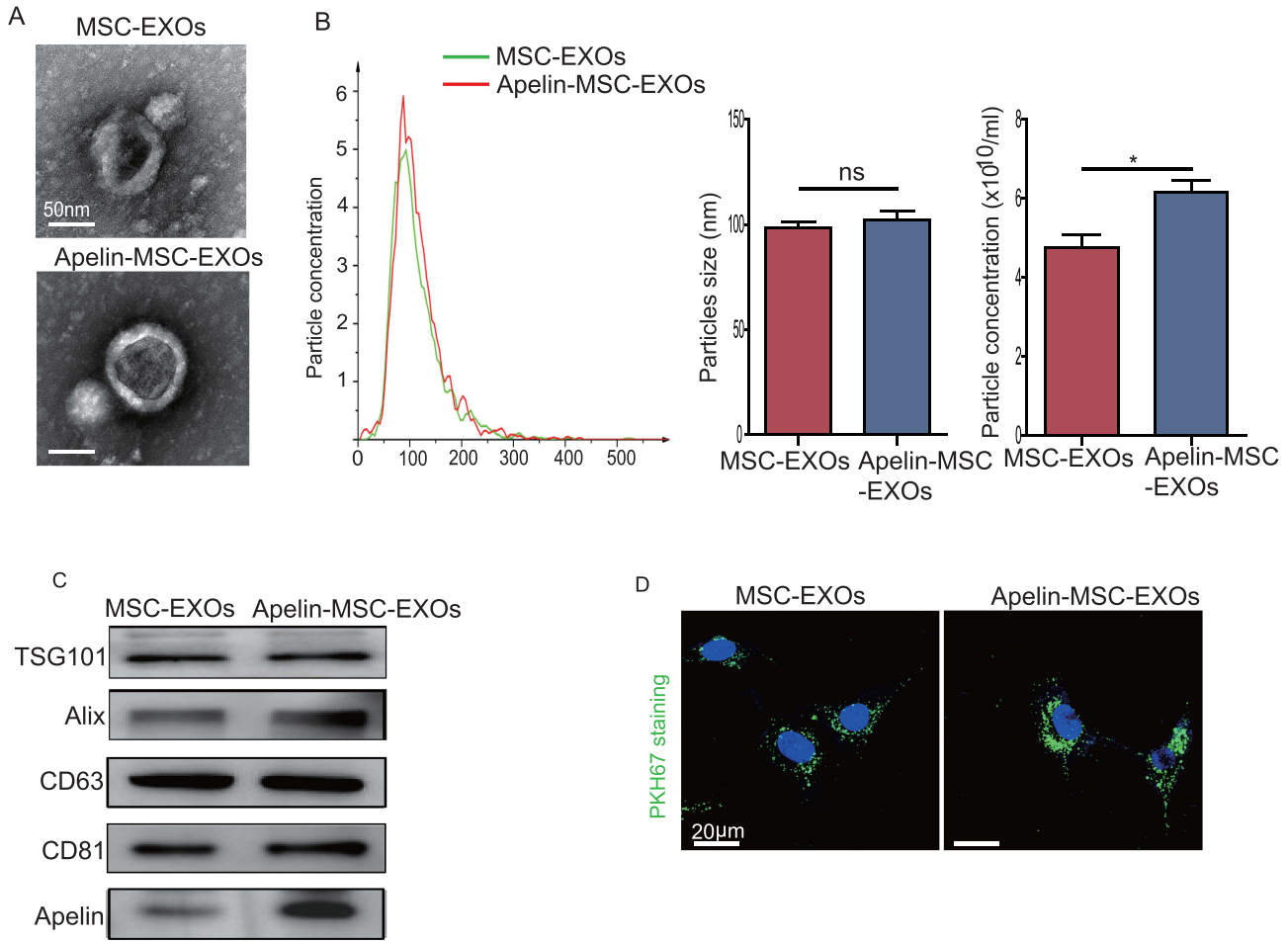

Figure 1 Characterization of MSC-EXOs and Apelin-MSC-EXOs. (**A**) MSC-EXOs and Apelin-MSC-EXOs showed cup-shaped morphology when examined by TEM. (**B**) NTA assay revealed particle size distribution and particle concentration of MSC-EXOs and Apelin-MSC-EXOs. Data are expressed as mean ± SEM. *$p < 0.05$, ns=not significant. (**C**) Western blotting showed MSC-EXOs and Apelin-MSC-EXOs expressed exosomal surface markers CD81, CD63, Alix, TSG101 and Apelin. (**D**) Representative confocal images demonstrate the uptake of labeled- MSC-EXOs and Apelin-MSC-EXOs by NMCs.

group and further alleviated in the Apelin-MSC-EXO group (Figure 2D). Collectively, these data showed that Apelin-MSC-EXO transplantation attenuated CLP-induced myocardial injury and heart dysfunction in a mouse model.

Apelin-MSC-EXO Transplantation Ameliorated Cardiomyocyte Pyroptosis in SMD Mice

Our previous study revealed that NLRP3 inflammasome-mediated cardiomyocyte pyroptosis led to SMD.[27] We aimed to determine whether Apelin-MSC-EXO transplantation could improve cardiac function by inhibiting cardiomyocyte pyroptosis. TUNEL staining showed that the number of TUNEL positive cardiomyocytes was greatly increased in the CLP group compared with the sham group but decreased following MSC-EXO treatment (Figure 3A and B). Furthermore, compared with the MSC-EXOs group, the ratio of TUNEL positive cardiomyocytes was decreased in the Apelin-MSC-EXOs group (Figure 3A and B). Western blotting showed that compared with the sham group, the protein level of ASC, NLRP3, the ratio of GSDMD-NT/GSDMD, Caspase-1/pro-Caspase-1, IL-1β and IL-18 were enhanced in the heart tissue of CLP-treated mice but dramatically decreased in the MSC-EXO group and Apelin-MSC-EXO group (Figure 3C). More importantly, the expression of pyroptosis-related markers was much lower in the Apelin-MSC-EXO group than MSC-EXO group, indicating that Apelin-MSC-EXOs were superior to MSC-EXOs in ameliorating cardiomyocyte pyroptosis in SMD mice (Figure 3C). Collectively, these results indicated that Apelin-MSC-EXO Transplantation ameliorated cardiomyocyte pyroptosis in SMD mice.

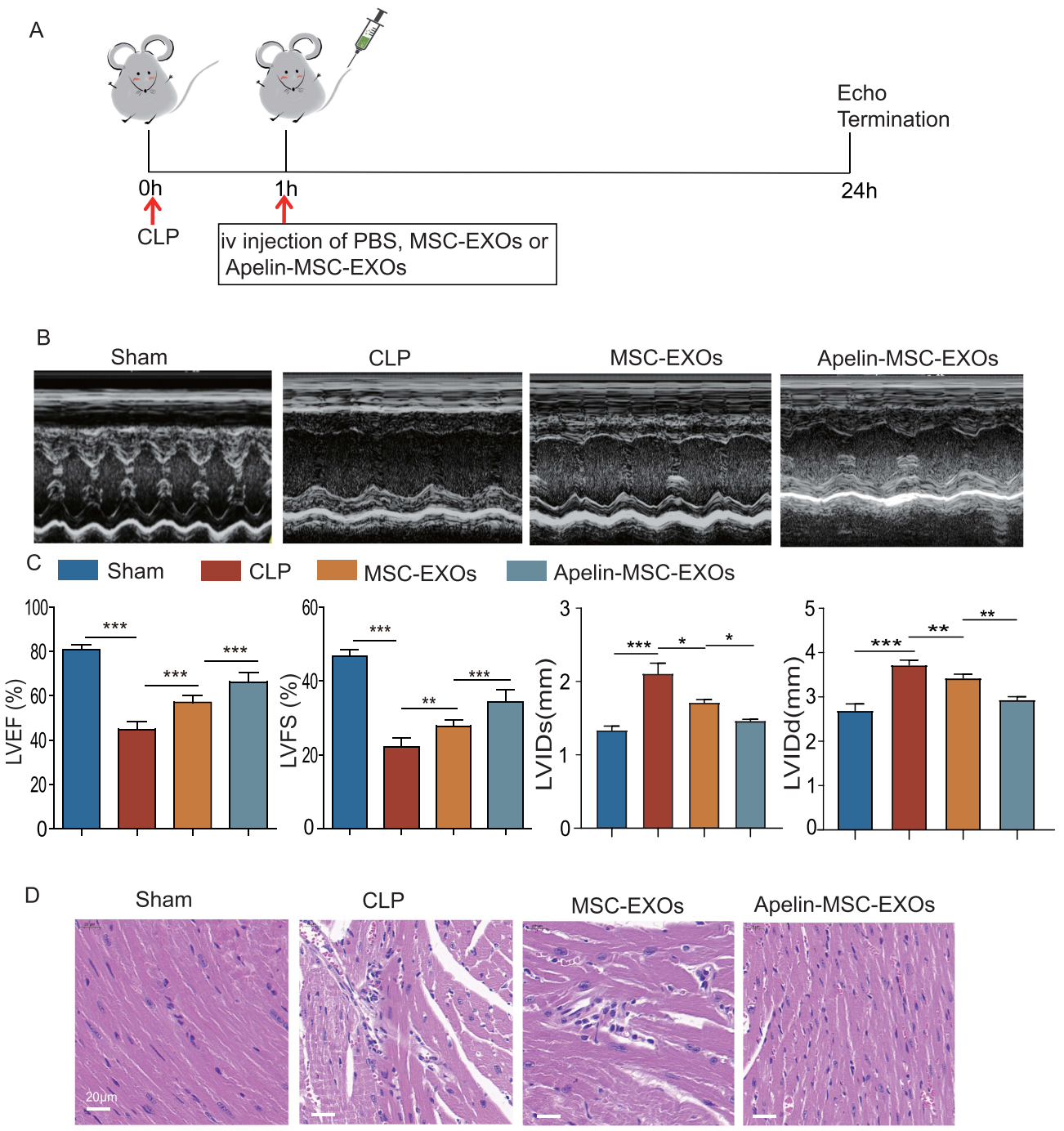

Figure 2 Transplantation of Apelin-MSC-EXOs improved cardiac function in SMD mice. (**A**)Schematic chart showing the creation of a mouse model of SMD using CLP and administration of PBS, MSC-EXOs or Apelin-MSC-EXOs. (**B**) Representative echocardiographic images were captured at 24h after CLP operation in mice treated with PBS, MSC-EXOs or Apelin-MSC-EXOs or control mice. (**C**) The LVIDd, LVIDs, LVEF and LVFS were analyzed at 24h in control mice or mice with CLP that received PBS, MSC-EXOs or Apelin-MSC-EXOs treatment. Data are expressed as mean ± SEM. n = 6 mice for each group, $*p < 0.05$, $**p < 0.01$, $***p < 0.001$. (**D**) Representative images of HE staining showing myocardial histological changes in CLP mice treated with PBS, MSC-EXOs or Apelin-MSC-EXOs and control mice.

Apelin-MSC-EXO Treatment Inhibited LPS-Induced Cardiomyocyte Pyroptosis

To examine the protective effects of Apelin-MSC-EXOs on cardiomyocyte pyroptosis in vitro, we incubated NMCs with MSC-EXOs or Apelin-MSC-EXOs for 24h under LPS conditions. LPS challenge significantly increased TUNEL positive cells (Figure 4A and B) and the protein level of ASC, NLRP3, the ratio of GSDMD-NT/GSDMD and Caspase-1/pro-Caspase-1 in NMCs (Figure 4C). These phenomena were partially reversed by treatment with MSC-EXOs or Apelin-

https://doi.org/10.2147/IJN.S498770

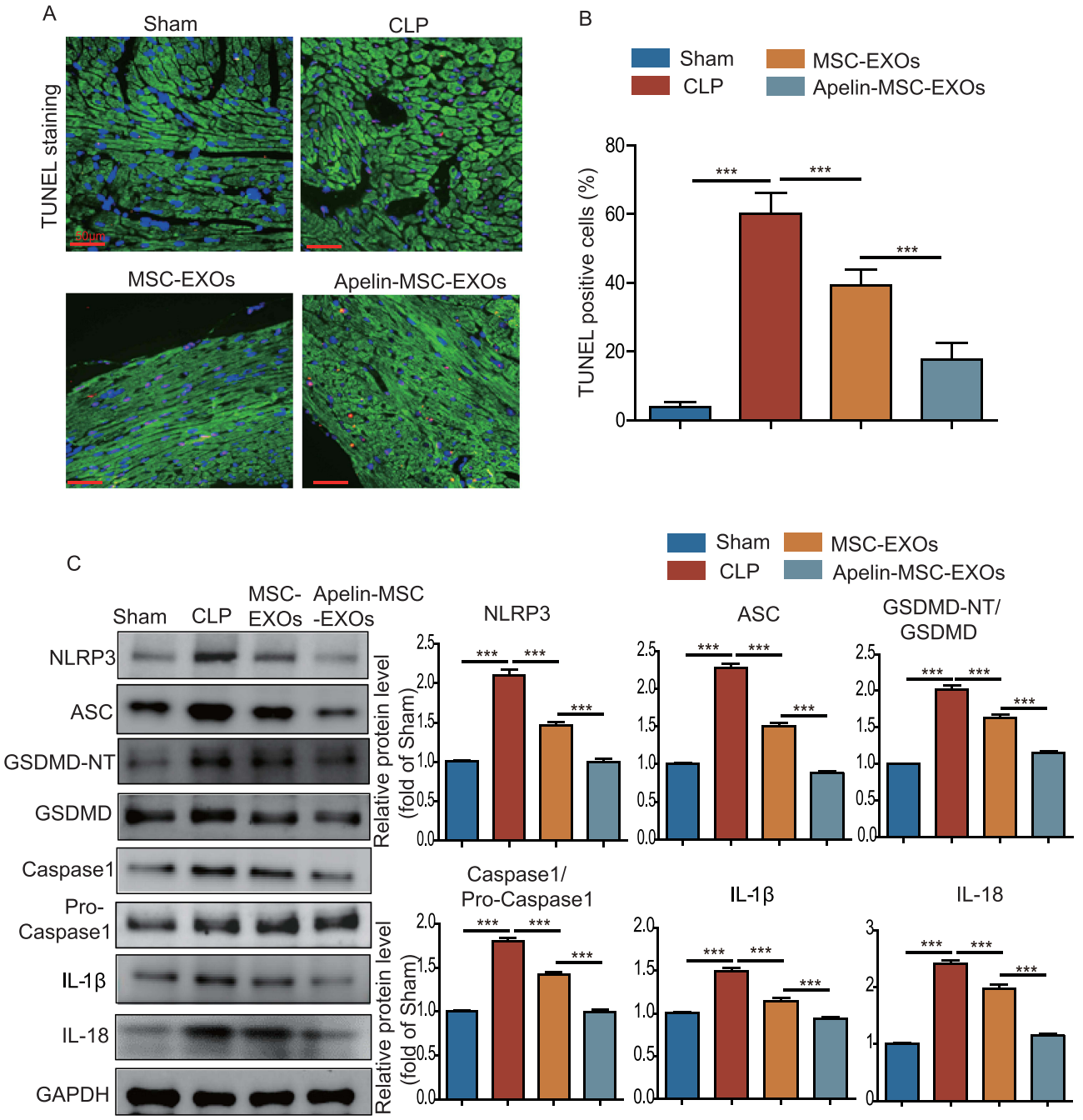

Figure 3 Transplantation of Apelin-MSC-EXOs ameliorated cardiomyocyte pyroptosis in SMD mice. (**A**) Representative images of Troponin and TUNEL double staining in the heart of CLP mice that received PBS, MSC-EXOs or Apelin-MSC-EXOs treatment and control mice. (**B**) Quantitative measurement of TUNEL positive cardiomyocytes in the heart of CLP mice that received PBS, MSC-EXO or Apelin-MSC-EXO treatment and control mice. (**C**) Western blotting and quantitative measurement of the protein level of NLRP3, ASC, the ratio of Caspase-1/pro-Caspase-1, GSDMD-NT/GSDMD as well as IL-1β and IL-18 in the heart of CLP mice that received PBS, MSC-EXO or Apelin-MSC-EXO treatment and control mice. Data are expressed as mean ± SEM. n = 6 mice for each group, ***$p < 0.001$.

MSC-EXOs (Figure 4A-C). Furthermore, compared with the MSC-EXOs group, the number of TUNEL positive NMCs and the protein level of ASC, NLRP3, the ratio of GSDMD-NT/GSDMD and Caspase-1/pro-Caspase-1 was greatly downregulated in the Apelin-MSC-EXOs group (Figure 4A-C). Nonetheless these beneficial effects of MSC-EXOs and Apelin-MSC-EXOs were largely reversed by NLRP3 inflammasome activator nigericin (Nig) (10 μM for 6 h). Overall, these results suggested that Apelin-MSC-EXO treatment attenuated LPS-induced cardiomyocyte pyroptosis in vivo.

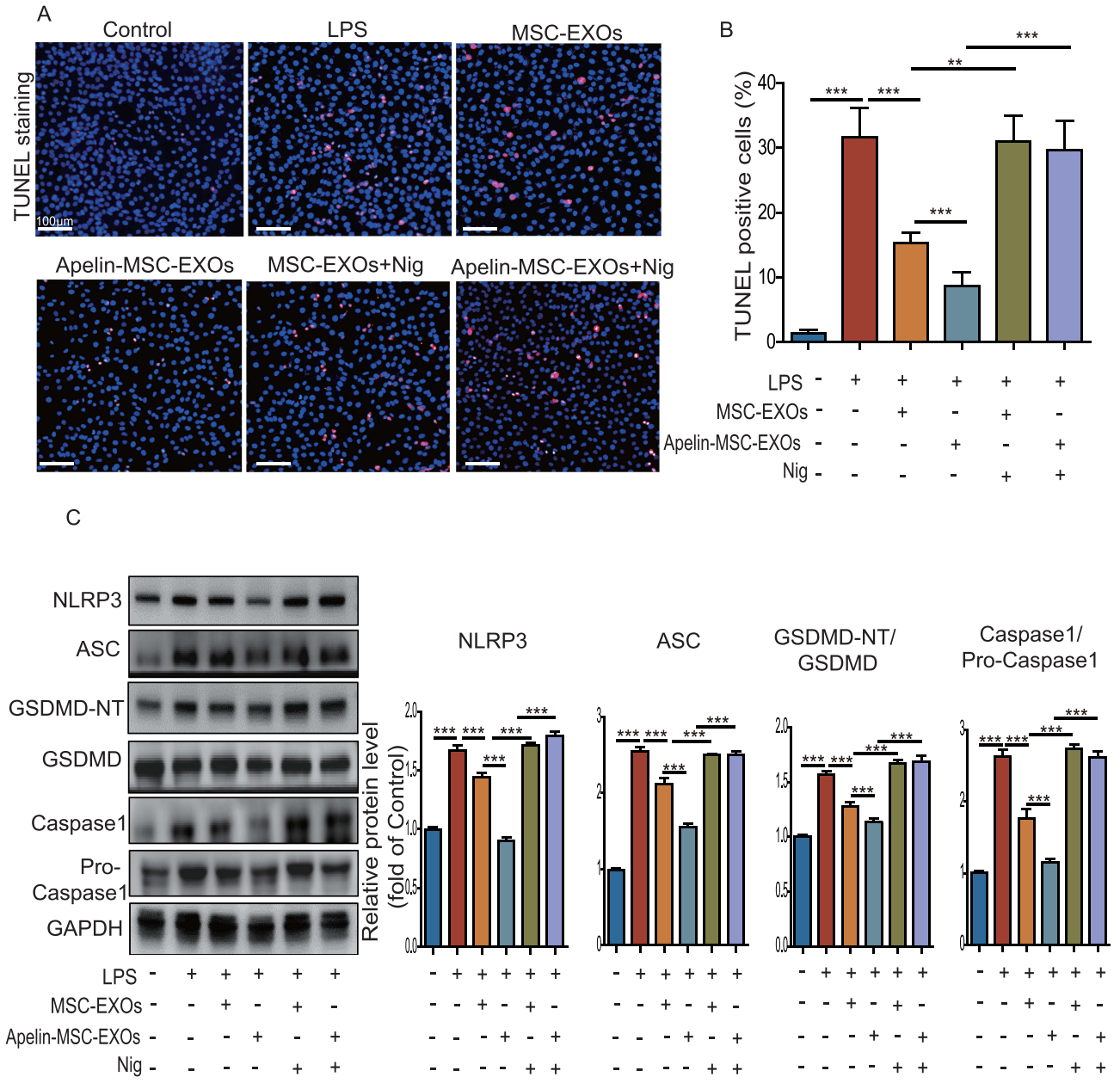

Figure 4 Apelin-MSC-EXOs treatment inhibited cardiomyocyte pyroptosis induced by LPS in vivo. (**A**) Representative TUNEL staining images in control, LPS, LPS+MSC-EXO, LPS+Apelin-MSC-EXO, LPS+MSC-EXOs+Nig, and LPS+ Apelin-MSC-EXO+ Nig-treated NMCs. (**B**) Quantitative measurement of TUNEL positive NMCs from the different groups. (**C**)Western blotting and quantitative measurement of the protein level of NLRP3, ASC, the ratio of Caspase-1/pro-Caspase-1 and GSDMD-NT/GSDMD in control, LPS, LPS+MSC-EXO, LPS+Apelin-MSC-EXO, LPS+MSC-EXOs+Nig, and LPS+Apelin-MSC-EXO+ Nig-treated NMCs. n = 3 biological replicates for each group. Data are expressed as mean ± SEM. $^{**}p < 0.01$, $^{***}p < 0.001$.

miR-34a-5p Delivered by Apelin-MSC-EXOs Inhibited Cardiomyocyte Pyroptosis

Since it is established that MSC-EXOs exert their cardioprotective effects via delivery of specific miRNAs,[30,31] we subsequently screened the potential candidate miRNAs in MSC-EXOs and Apelin-MSC-EXOs using miRNA–seq. The different expression of miRNAs between MSC-EXOs and Apelin-MSC-EXOs was analyzed and is shown in Figure 5A. We searched the literature and determined that the expression of miR-34a-5p was closely associated with cardiovascular diseases.[32,33] We thus performed RT-qPCR and found that the level of miR-34a-5p in Apelin-MSC-EXOs was much higher than that in MSC-EXOs (Figure 5B). To determine whether Apelin-MSC-EXOs could deliver miR-34a-5p to regulate cardiomyocyte pyroptosis under LPS challenge, Apelin-MSCs were manipulated with miR-34a-5p inhibitor to extract miR-34a-5p^{KD}-Apelin-MSC-EXOs. RT-qPCR results indicated either that Apelin-MSCs manipulated with miR-34a-5p inhibitor or

https://doi.org/10.2147/IJN.S498770

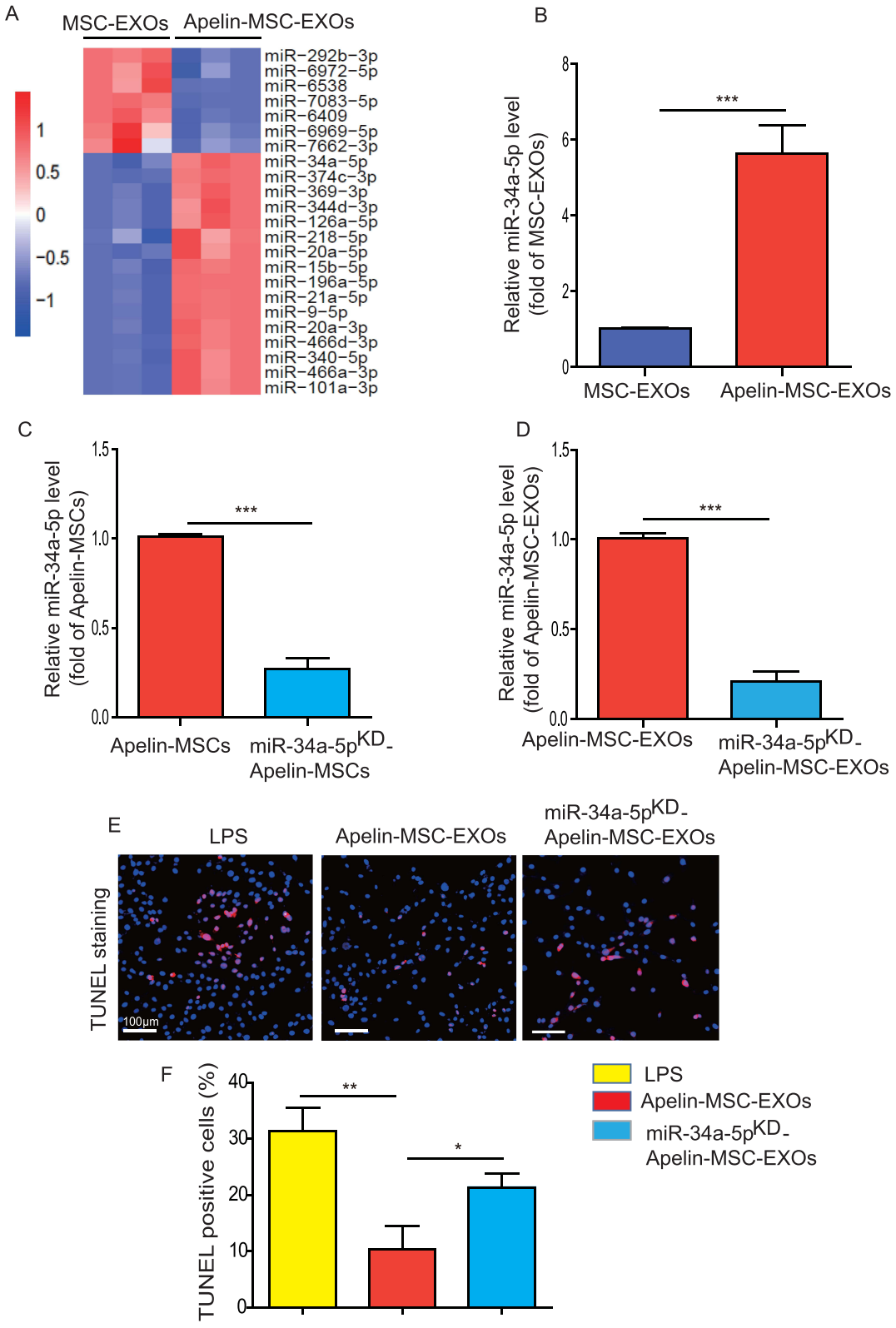

Figure 5 miR-34a-5p delivered by Apelin-MSC-EXOs inhibited cardiomyocyte pyroptosis. (**A**) The results of RNA-seq analysis revealed the differential expression of miRNAs between MSC-EXOs and Apelin-MSC-EXOs. (**B**) The expression level of miR-34a-5p in Apelin-MSC-EXOs was determined by qPCR. (**C**) The expression level of miR-34a-5p in Apelin-MSCs and miR-34a-5p^{KD}-Apelin-MSCs was evaluated by qPCR. (**D**) The expression level of miR-34a-5p in Apelin-MSC-EXOs and miR-34-5p^{KD}-Apelin-MSC-EXOs was validated by qPCR. (**E**) Representative images of TUNEL staining in NMCs treated with Apelin-MSC-EXOs or miR-34-5p^{KD}-Apelin-MSC-EXOs under LPS challenge. (**F**) Quantitative measurement of TUNEL staining in NMCs treated with Apelin-MSC-EXOs or miR-34-5p^{KD}-Apelin-MSC-EXOs under LPS challenge. n=3 biological replicates for each group. Data are expressed as mean ± SEM. *$p < 0.05$, **$p < 0.01$, ***$p < 0.001$.

https://doi.org/10.2147/IJN.S498770

the derived EXOs exhibited a reduced level of miR-34a-5p (Figure 5C and D). Next, we evaluated the effects of miR-34a-5p^{KD}-Apelin-MSC-EXOs on LPS-induced NMCs pyroptosis. Compared with the LPS group, the number of TUNEL positive NMCs was greatly downregulated in the Apelin-MSC-EXO group but upregulated in the miR-34a-5p^{KD}-Apelin-MSC-EXO group (Figure 5E and F). These results confirmed that Apelin-MSC-EXOs prevented NMC pyroptosis induced by LPS via delivery of miR-34a-5p.

miR-34a-5p Delivered by Apelin-MSC-EXOs Inhibited Cardiomyocyte Pyroptosis via Regulation of the HMGB1/AMPK Axis

TargetScan predicted HMGB1 as a potential downstream molecule of miR-34a-5p (Figure 6A). Subsequently, NMCs were used to validate the binding relationship between the 3′UTR target region of HMGB1 and miR-34a-5p. The luciferase activity revealed that compared with miR control, miR-34a-5p mimic treatment downregulated luciferase activity of the HMGB1-WT vector but had no impact on luciferase activity of the HMGB1-mutant vector in NMCs (Figure 6B). Next, to determine the relationship between HMGB1and miR-34a-5p, we first treated NMCs with miR-34a-5p mimic, miR-34a-5p inhibitor or miR control. The expression of miR-34a-5p was greatly enhanced in miR-34a-5p mimic-treated NMCs but decreased in miR-34a-5p inhibitor-treated NMCs (Figure 6C). Results from qPCR and Western blotting showed that the level of HMGB1 mRNA and protein was downregulated in miR-34a-5p mimic-treated NMCs but up-regulated in miR-34a-5p inhibitor-treated NMCs (Figure 6D and E). It has been well documented that HMGB1 is involved in regulating heart dysfunction via mediation of the AMPK pathway.[34,35] Therefore, we aimed to determine whether Apelin-MSC-EXOs protected against SMD by inhibition of cardiomyocyte pyroptosis by regulating the HMGB1/AMPK axis. We first evaluated the expression of HMGB1, p-AMPK in SMD mice that received MSC-EXO or Apelin-MSC-EXO treatment. As shown in Figure S1, the expression of HMGB1 was remarkably increased in the CLP group compared with the sham group but reduced in the MSC-EXO and Apelin-MSC-EXO groups, to a greater extent in the latter (Figure S1). In contrast, the level of p-AMPK was decreased in the CLP group but increased in MSC-EXO group and Apelin-MSC-EXO group, again to a greater extent in the latter (Figure S1). To verify that exosomal miR-34a-5p in Apelin-MSC-EXOs ameliorated cardiomyocyte pyroptosis via inhibition of the HMGB1/AMPK axis, we treated NMCs with miR-34a-5p^{KD}-Apelin-MSC-EXOs under LPS. We showed that Apelin-MSC-EXO treatment downregulated the level of HMGB1, ASC, NLRP3, the ratio of GSDMD-NT/GSDMD and Caspase-1/pro-Caspase-1 but enhanced the level of p-AMPK/AMPK in LPS-treated NMCs (Figure 6F). Nonetheless the expression of HMGB1, ASC, NLRP3, the ratio of GSDMD-NT/GSDMD and Caspase-1/pro-Caspase-1 was upregulated whereas the level of p-AMPK/AMPK was downregulated in the miR-34a-5p^{KD}-Apelin-MSC-EXO group compared with the Apelin-MSC-EXOs group. These effects of Apelin-MSC-EXOs on LPS treated-NMCs were greatly abrogated by Compound C (AMPK inhibitor) (Figure 6F). Collectively, these data demonstrated that miR-34a-5p enriched in Apelin-MSC-EXOs inhibited cardiomyocyte pyroptosis via regulation of the HMGB1/AMPK axis.

Knockdown of miR-34a-5p Downregulated Apelin-MSC-EXO-Mediated Cardioprotective Effects in SMD Mice

To confirm whether miR-34a-5p were responsible for the cardioprotective effects of Apelin-MSC-EXOs on SMD, we transplanted miR-34a-5p^{KD}-Apelin-MSC-EXOs into a mouse model of SMD at 1h post CLP surgery. At 24h post operation, LVEF and LVFS were reduced in the miR-34a-5p^{KD}-Apelin-MSC-EXOs group compared with the Apelin-MSC-EXOs group (Figure 7A and B). In contrast, LVIDs and LVIDd were increased in the miR-34a-5p^{KD}-Apelin-MSC-EXO group compared with the Apelin-MSC-EXO group (Figure 7A and B). HE staining showed that compared with the Apelin-MSC-EXO group, inflammatory infiltration and broken myocardial fibers were upregulated in the miR-34a-5p^{KD}-Apelin-MSC-EXO group (Figure 7C). The TUNEL assay demonstrated that compared with the Apelin-MSC-EXO group, the ratio of TUNEL positive cardiomyocytes in mouse myocardial tissue was notably enhanced in the miR-34a-5p^{KD}-Apelin-MSC-EXO group (Figure 7D and E). Moreover, Western blotting revealed that the level of p-AMPK was downregulated whereas the protein level of HMGB1, ASC, NLRP3, the ratio of GSDMD-NT/GSDMD, Caspase-1/pro-Caspase-1, IL-1β and IL-18 was upregulated in the miR-34a-5p^{KD}-Apelin-MSC-EXO group compared with the Apelin-MSC-EXO group (Figure 7F). Collectively, these

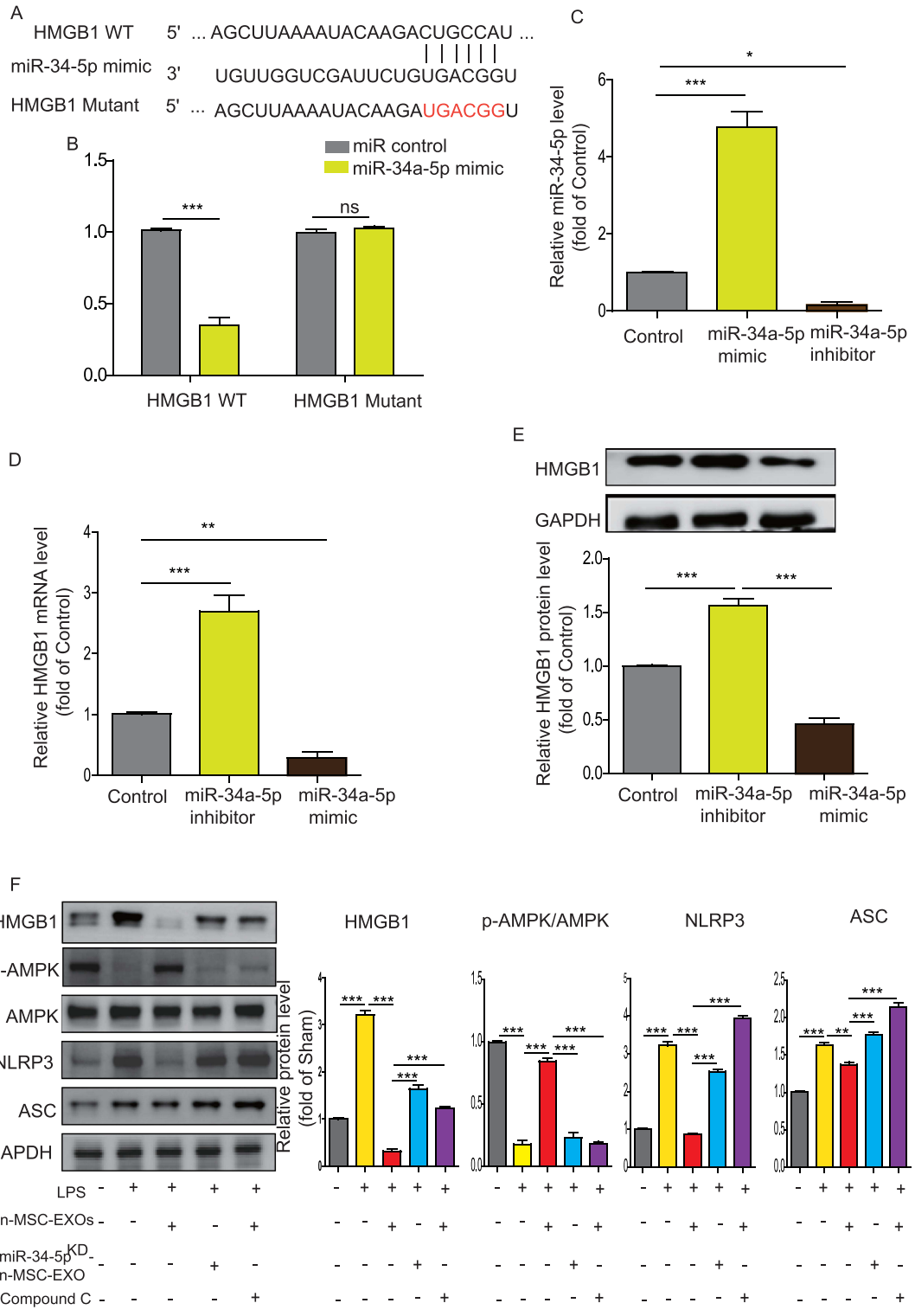

Figure 6 miR-34a-5p delivered by Apelin-MSC-EXOs inhibited cardiomyocyte pyroptosis via regulation of the HMGB1/AMPK pathway. (**A**) Bioinformatics analysis predicted the binding sites between 3'UTR target region of HMGB1 and miR-34a-5p. (**B**) Luciferase activity of the HMGB1-WT and HMGB1-mutant in NMCs following miR-34a-5p mimic transfection. (**C**) The level of miR-34a-5p in NMCs treated with control, miR-34a-5p mimic or miR-34a-5p inhibitor was determined by qPCR. (**D**) The level of HMGB1 in NMCs treated with control, miR-34a-5p mimic or miR-34a-5p inhibitor was measured by qPCR. (**E**) The level of HMGB1 in NMCs treated with control, miR-34a-5p mimic or miR-34a-5p inhibitor was examined by Western blotting. (**F**) Western blotting and quantitative measurement of the level of HMGB1, p-AMPK/AMPK, NLRP3, ASC, the ratio of Caspase-1/pro-Caspase-1 and GSDMD-NT/GSDMD in control, LPS, LPS+Apelin-MSC-EXOs, LPS+ miR-34a-5p^{KD}-Apelin-MSC-EXOs and LPS+Apelin-MSC-EXOs+ Compound C treated NMCs. n = 3 biological replicates for each group. Data are expressed as mean ± SEM. *$p < 0.05$, **$p < 0.01$, ***$p < 0.001$, ns=not significant.

https://doi.org/10.2147/IJN.S498770

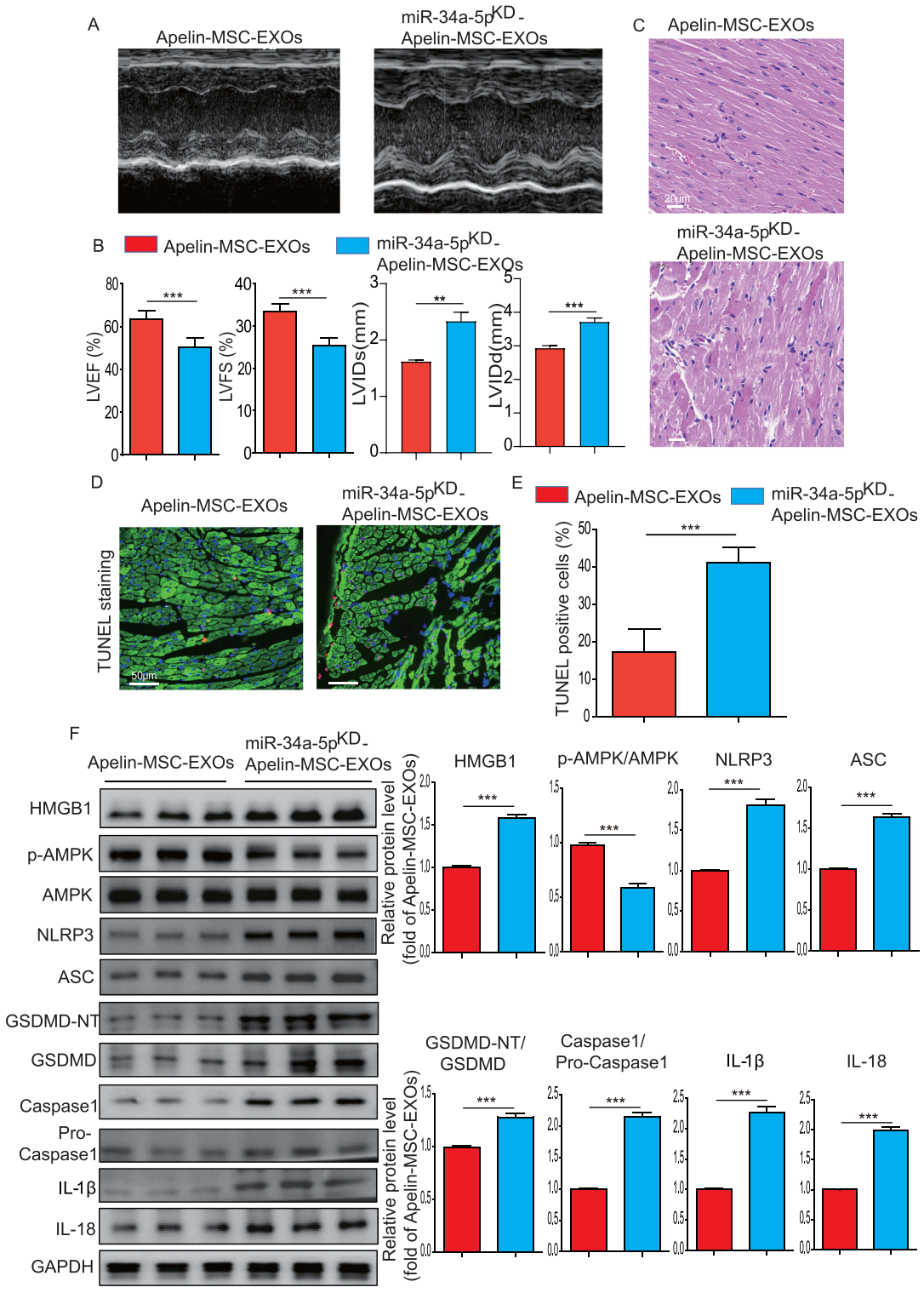

Figure 7 Knockdown of miR-34a-5p reduced Apelin-MSC-EXO-mediated cardioprotective effects in SMD mice. (**A**) Representative echocardiographic images captured at 24h after CLP operation in mice that received Apelin-MSC-EXOs or miR-34a-5p^{KD}-Apelin-MSC-EXOs. (**B**) The LVIDs, LVIDd, LVEF and LVFS were analyzed at 24h after CLP operation in mice that received Apelin-MSC-EXOs or miR-34a-5p^{KD}-Apelin-MSC-EXOs. (**C**) Representative images of HE staining showing myocardial histological changes in CLP mice treated with Apelin-MSC-EXOs or miR-34a-5p^{KD}-Apelin-MSC-EXOs. (**D**) Representative images of Troponin and TUNEL double staining in the heart of CLP mice treated with Apelin-MSC-EXOs or miR-34a-5p^{KD}-Apelin-MSC-EXOs. (**E**) Quantitative measurement of TUNEL positive cardiomyocytes in the heart of CLP mice treated with Apelin-MSC-EXOs or miR-34a-5p^{KD}-Apelin-MSC-EXOs. (**F**) Western blotting and quantitative measurement of the level of HMGB1, p-AMPK/AMPK, NLRP3, ASC, the ratio of Caspase-1/pro-Caspase-1 and GSDMD-NT/GSDMD as well as IL-1β and IL-18 in the heart of CLP mice treated with Apelin-MSC-EXOs or miR-34a-5p^{KD}-Apelin-MSC-EXOs. Data are expressed as mean ± SEM. n=6 mice for each group, $^{**}p < 0.01$, $^{***}p < 0.001$.

https://doi.org/10.2147/IJN.S498770

data showed that downregulation of miR-34a-5p expression in Apelin-MSC-EXOs reduced their cardioprotective effects in SMD.

Discussion

Several major findings were highlighted in the current study. First, compared with MSC-EXOs, Apelin-MSC-EXO administration exerted superior cardioprotective effects against SMD in CLP-treated mice. Second, Apelin-MSC-EXOs alleviated myocardial impairment by attenuating NLRP3-mediated cardiomyocyte pyroptosis. Third, the cardioprotective effects of Apelin-MSC-EXOs on SMD were largely attributed to the high level of miR-34a-5p that ameliorated cardiomyocyte pyroptosis by targeting the HMGB1/AMPK axis. Our study showed that Apelin-MSC-EXOs present a new therapeutic approach for SMD treatment.

MSC-EXO-based therapy has become a popular cell-free treatment for sepsis and sepsis-related diseases due to their lower immunogenicity, less tumorigenicity and ability to transport various bioactive components.[36–38] It has been documented that treatment with sweroside-functionalized MSC-EXOs ameliorated heart injury via downregulation of oxidative stress and cardiomyocyte apoptosis in LPS-treated rats.[39] Zhou et al reported that transplantation of EXOs isolated from human umbilical cord MSCs ameliorated cardiac injury in SMD mice by improving mitochondrial Ca^{2+} efflux in cardiomyocytes through delivery of PINK1 mRNA.[40] In our study, MSC-EXO transplantation significantly improved heart function in CLP-treated mice. More importantly, administration of MSC-EXOs effectively inhibited cardiomyocyte pyroptosis in CLP-treated mice and LPS-treated NMCs. Although administration of MSC-EXOs has shown great advantages in improving cardiac function following sepsis, how to obtain more EXOs with stronger protective effects to target SMD effectively requires further investigation. There is accumulating evidence that pretreatment with hypoxia, drugs or cytokines can significantly improve the protective effects of MSC-EXOs against sepsis,[41,42] providing more possibilities for future SMD treatment. It has been shown that LPS pretreatment increases the protective efficacy of MSC-EXOs in CLP-induced septic liver injury via regulation of macrophage STING signaling by transport of ATG2B.[43] Therefore, identification of a suitable drug to pre-treat MSCs and enhance the protective effects of MSCs-EXOs on SMD is urgently needed. Our previous studies found that Apelin pretreatment not only rejuvenated the aged MSCs but also improved their cardioprotective effects following transplantation in a mouse model of myocardial infarction by augmenting the paracrine effects.[15,44] We also found that Apelin ameliorated SMD by downregulating NLRP3-mediated pyroptosis of cardiomyocytes.[26] Based on our previous results and findings from the current study, we hypothesized that Apelin pretreatment could enhance the cardioprotective efficacy of MSC-EXOs on SMD by ameliorating cardiomyocyte pyroptosis. As predicted, administration of Apelin-MSC-EXOs was superior to MSC-EXOs in improving heart function in a mouse model of SMD via amelioration of cardiomyocyte pyroptosis.

Since we revealed that transplantation of Apelin-MSC-EXOs had superior therapeutic efficacy in SMD than MSC-EXOs, it would be interesting to determine which biological substance is responsible. There is increasing evidence that MSC-EXOs exert their therapeutic efficacy for heart repair/regeneration via delivery of their active molecule miRNAs by regulating cardiomyocyte viability, angiogenesis and inflammation.[45–47] It has been reported that transplantation of MSC-EXOs alleviated myocardial impairment, cardiomyocyte apoptosis and inflammatory infiltration in CLP-treated mice via conveying miR-141 by targeting the PTEN/β-catenin pathway.[48] To identify the key miRNA that accounts for the heightened therapeutic efficacy of Apelin-MSC-EXOs on SMD, RNA-seq was performed to identify the key miRNAs between Apelin-MSC-EXOs and MSC-EXOs. Among the miRNAs highly enriched in Apelin-MSC-EXOs, miR-34a-5p has attracted huge attention. miRNA–seq showed that miR-34a-5p is highly expressed in Apelin-MSC-EXOs. RT-qPCR showed that the level of miR-34a-5p in Apelin-MSC-EXOs was much higher than that in MSC-EXOs. Furthermore, miR-34-5p inhibited fibrogenesis of cardiac fibroblasts by reducing ROCK1 and improved heart function following myocardial infarction, suggesting a protective role of miR-34-5p in heart repair.[49] Here, we found that miR-34a-5p knockdown in Apelin-MSC-EXOs downregulated their capacity to ameliorate cardiomyocyte pyroptosis, thereby reducing their therapeutic efficacy for SMD, suggesting that the protective effects of Apelin-MSC-EXOs were partially attributed to the high level of miR-34a-5p. Next, we identified HMGB1 as a key target of miR-34a-5p via bioinformatics analysis and luciferase activity assay. HMGB1 acts as an inflammatory and immunomodulatory factor involved in regulating a variety of diseases by activating NLRP3 inflammasome.[50,51] It has been demonstrated that LPS-treated

macrophage HMGB1-enriched extracellular vesicles stimulated hepatocyte pyroptosis via activation of the NLRP3 inflammasome.[52] Notably, HMGB1 overexpression can lead to overactivation of NLRP3 inflammasome via mediation of the AMPK signaling pathway.[53] Here, the protein level of HMGB1 as well as NLRP3 and pyroptosis markers was significantly up-regulated and p-AMPK was greatly decreased in LPS-treated NMCs and the heart tissues from CLP-treated mice. Nonetheless these effects were partially abrogated in the Apelin-MSC-EXO treatment group. More importantly, the Apelin-MSC-EXO-inhibited LPS-induced NMC pyroptosis was largely abrogated by Compound C. Collectively, our study showed that exosomal miR-34a-5p in Apelin-MSC-EXOs attenuates cardiomyocyte pyroptosis in an SMD model in vitro and in vivo via regulation of the HMGB1/AMPK axis.

There are some limitations that should be acknowledged in this study. First, in addition to HMGB1, whether Apelin-MSC-exosomal miR-34a-5p inhibits cardiomyocyte pyroptosis in a mouse model of SMD via regulation of other targets warrants investigation. Second, in addition to miR-34a-5p, whether other noncoding RNAs or proteins that are highly expressed in Apelin-MSC-EXOs exert cardioprotective effects against SMD requires further investigation. Third, how Apelin pretreatment can enhance the level of miR-34a-5p in MSC-EXOs was not determined in the current study. Fourth, whether miR-34a-5p has potential as an effective biomarker for a diagnosis of SMD in humans will be explored in follow-up studies.

In conclusion, our study showed that EXOs derived from Apelin-primed MSCs exhibited a superior therapeutic efficacy in SMD and was mainly attributed to increased expression of miR-34a-5p. Moreover, Apelin-MSC-exosomal miR-34a-5p ameliorated cardiomyocyte pyroptosis via mediation of the HMGB1/AMPK axis. This study presents a new perspective to treatments for SMD.

Data Sharing Statement

Data are available on request from the corresponding authors.

Acknowledgment

The authors thank Dr. Xiaoting Liang for providing MSCs.

Funding

This research was financially supported by NSFC (No. 82072139 to B. Hu, No. 82270253 to Y. Zhang; No. 82072225 to X. Li), the Natural Science Foundation of Guangdong Province (No. 2022B1515020104 to Y. Zhang), Guangdong Provincial People's Hospital for Distinguished Young Scholars (No. KY0120220132 to Y. Zhang) and the National key research and development program intergovernmental key projects (No. 2023YFE0114300).

Disclosure

The authors declare no conflicts of interest.

References

1. Rudd KE, Johnson SC, Agesa KM. et al. Global, regional, and national sepsis incidence and mortality, 1990-2017: analysis for the global burden of disease study. *Lancet*. 2020;395(10219):200–211. doi:10.1016/S0140-6736(19)32989-7
2. Cicchinelli S, Pignataro G, Gemma S, et al. PAMPs and DAMPs in sepsis: a review of their molecular features and potential clinical implications. *Int J Mol Sci*. 2024;25(2):962. doi:10.3390/ijms25020962
3. Du X, Zhang M, Zhou H, et al. Decoy nanozymes enable multitarget blockade of proinflammatory cascades for the treatment of multi-drug-resistant bacterial sepsis. *Research*. 2022;2022:9767643. doi:10.34133/2022/9767643
4. Kakihana Y, Ito T, Nakahara M, Yamaguchi K, Yasuda T. Sepsis-induced myocardial dysfunction: pathophysiology and management. *J Intens Care*. 2016;4(1):22. doi:10.1186/s40560-016-0148-1
5. Joshi S, Kundu S, Priya VV, Kulhari U, Mugale MN, Sahu BD. Anti-inflammatory activity of carvacrol protects the heart from lipopolysaccharide-induced cardiac dysfunction by inhibiting pyroptosis via NLRP3/Caspase1/Gasdermin D signaling axis. *Life Sci*. 2023;324:121743. doi:10.1016/j.lfs.2023.121743
6. Wang Z, Wu Q, Nie X, Guo J, Yang C. Combination therapy with milrinone and esmolol for heart protection in patients with severe sepsis: a prospective, randomized trial. *Clin. Drug Invest.* 2015;35(11):707–716. doi:10.1007/s40261-015-0325-3
7. Zhu B, Jiang J, Yu H, Huang L, Zhou D. Effect of norepinephrine, vasopressin, and dopamine for survivals of the elderly with sepsis and pre-existing heart failure. *Sci Rep*. 2024;14(1):1948. doi:10.1038/s41598-024-52514-5

8. Wang X, Gu H, Qin D, et al. Exosomal miR-223 contributes to mesenchymal stem cell-elicited cardioprotection in polymicrobial sepsis. *Sci Rep*. 2015;5(1):13721. doi:10.1038/srep13721
9. Li J, Jiang R, Hou Y, Lin A. Mesenchymal stem cells-derived exosomes prevent sepsis-induced myocardial injury by a CircRTN4/miR-497-5p/MG53 pathway. *Biochem. Biophys. Res. Commun.* 2022;618:133–140. doi:10.1016/j.bbrc.2022.05.094
10. Xu J, Xiong YY, Li Q, et al. Optimization of timing and times for administration of atorvastatin-pretreated mesenchymal stem cells in a preclinical model of acute myocardial infarction. *Stem Cells Translational Med*. 2019;8(10):1068–1083. doi:10.1002/sctm.19-0013
11. Deng R, Liu Y, He H, et al. Haemin pre-treatment augments the cardiac protection of mesenchymal stem cells by inhibiting mitochondrial fission and improving survival. *J Cell & Mol Med*. 2020;24(1):431–440. doi:10.1111/jcmm.14747
12. Lee D, Cheng R, Nguyen T, et al. Characterization of apelin, the ligand for the APJ receptor. *J Neurochem*. 2000;74(1):34–41. doi:10.1046/j.1471-4159.2000.0740034.x
13. Chapman FA, Maguire JJ, Newby DE, et al. Targeting the apelin system for the treatment of cardiovascular diseases. *Cardiovasc Res*. 2023;119(17):2683–2696. doi:10.1093/cvr/cvad171
14. Gao S, Chen H. Therapeutic potential of apelin and Elabela in cardiovascular disease. *Biomed Pharmacother*. 2023;166:115268. doi:10.1016/j.biopha.2023.115268
15. Chandrasekaran B, O DAR, Mcdonagh T. The role of apelin in cardiovascular function and heart failure. *EurJ Heart Failure*. 2008;10(8):725–732. doi:10.1016/j.ejheart.2008.06.002
16. Chen G, Liang X, Han Q, et al. Apelin-13 pretreatment promotes the cardioprotective effect of mesenchymal stem cells against myocardial infarction by improving their survival. *Stem Cells Int*. 2022;2022:3742678. doi:10.1155/2022/3742678
17. Lu C, Liu J, Escames G, et al. PIK3CG regulates NLRP3/GSDMD-mediated pyroptosis in septic myocardial injury. *Inflammation*. 2023;46(6):2416–2432.
18. Zheng X, Chen W, Gong F, Chen Y, Chen E. The role and mechanism of pyroptosis and potential therapeutic targets in sepsis: a review. *Front Immunol*. 2021;12:711939. doi:10.3389/fimmu.2021.711939
19. Song R, He S, Wu Y, Tan S. Pyroptosis in sepsis induced organ dysfunction. *Curr Res Trans Med*. 2023;72(2):103419. doi:10.1016/j.retram.2023.103419
20. Zeng C, Duan F, Hu J, et al. NLRP3 inflammasome-mediated pyroptosis contributes to the pathogenesis of non-ischemic dilated cardiomyopathy. *Redox Biol*. 2020;34:101523. doi:10.1016/j.redox.2020.101523
21. Hu J, Zeng C, Wei J, et al. The combination of Panax ginseng and Angelica sinensis alleviates ischemia brain injury by suppressing NLRP3 inflammasome activation and microglial pyroptosis. *Phytomedicine*. 2020;76:153251. doi:10.1016/j.phymed.2020.153251
22. Li X, Zhang P, Yin Z, et al. Caspase-1 and gasdermin D afford the optimal targets with distinct switching strategies in NLRP1b inflammasome-induced cell death. *Research*. 2022;2022:9838341. doi:10.34133/2022/9838341
23. Yang Z, Pan X, Wu X, et al. TREM-1 induces pyroptosis in cardiomyocytes by activating NLRP3 inflammasome through the SMC4/NEMO pathway. *FEBS J*. 2023;290(6):1549–1562. doi:10.1111/febs.16644
24. Zhang Y, Yu Z, Jiang D, et al. iPSC-MSCs with High Intrinsic MIRO1 and Sensitivity to TNF-α yield efficacious mitochondrial transfer to rescue anthracycline-induced cardiomyopathy. *Stem Cell Rep*. 2016;7(4):749–763. doi:10.1016/j.stemcr.2016.08.009
25. Zhang Y, Huang X, Sun T, et al. MicroRNA-19b-3p dysfunction of mesenchymal stem cell-derived exosomes from patients with abdominal aortic aneurysm impairs therapeutic efficacy. *J Nanobiotechnol*. 2023;21(1):135. doi:10.1186/s12951-023-01894-3
26. Zheng H, Liang X, Han Q, et al. Hemin enhances the cardioprotective effects of mesenchymal stem cell-derived exosomes against infarction via amelioration of cardiomyocyte senescence. *J Nanobiotechnol*. 2021;19(1):332. doi:10.1186/s12951-021-01077-y
27. Cao Z, Li W, Shao Z, et al. Apelin ameliorates sepsis-induced myocardial dysfunction via inhibition of NLRP3-mediated pyroptosis of cardiomyocytes. *Heliyon*. 2024;10(3):e24568. doi:10.1016/j.heliyon.2024.e24568
28. Tu GW, Ma JF, Li JK, et al. Exosome-derived from sepsis patients' blood promoted pyroptosis of cardiomyocytes by regulating miR-885-5p/HMBOX1. *Front Cardiovasc Med*. 2022;9:774193. doi:10.3389/fcvm.2022.774193
29. Zheng T, Li S, Zhang T, et al. Exosome-shuttled miR-150-5p from LPS-preconditioned mesenchymal stem cells down-regulate PI3K/Akt/mTOR pathway via Irs1 to enhance M2 macrophage polarization and confer protection against sepsis. *Front Immunol*. 2024;15:1397722. doi:10.3389/fimmu.2024.1397722
30. Liu Y, Wang M, Yu Y, et al. Advances in the study of exosomes derived from mesenchymal stem cells and cardiac cells for the treatment of myocardial infarction. *Cell Communication Signaling*. 2023;21(1):202. doi:10.1186/s12964-023-01227-9
31. Zhu W, Wang Q, Zhang J, et al. Exosomes derived from mir-214-3p overexpressing mesenchymal stem cells promote myocardial repair. *Biomater Res*. 2023;27(1):77. doi:10.1186/s40824-023-00410-w
32. Wenlan L, Zhongyuan X, Shaoqing L, Liying Z, Bo Z, Min L. MiR-34a-5p mediates sevoflurane preconditioning induced inhibition of hypoxia/reoxygenation injury through STX1A in cardiomyocytes. *Biomed Pharmacotherapie*. 2018;102:153–159. doi:10.1016/j.biopha.2018.03.002
33. Wang G, Yao J, Li Z, et al. miR-34a-5p inhibition alleviates intestinal ischemia/reperfusion-induced reactive oxygen species accumulation and apoptosis via activation of SIRT1 signaling. *Antioxid Redox Signal*. 2016;24(17):961–973. doi:10.1089/ars.2015.6492
34. Foglio E, Puddighinu G, Germani A, et al. HMGB1 inhibits apoptosis following MI and induces autophagy via mTORC1 Inhibition. *J Cell Physiol*. 2017;232(5):1135–1143. doi:10.1002/jcp.25576
35. Taskin E, Guven C, Tunc Kaya S, et al. Silencing HMGB1 expression inhibits Adriamycin's heart toxicity via TLR4 dependent manner through MAPK signal transduction. *J Buon*. 2020;25(1):554–565.
36. Wang X, Liu D, Zhang X, et al. Exosomes from adipose-derived mesenchymal stem cells alleviate sepsis-induced lung injury in mice by inhibiting the secretion of IL-27 in macrophages. *Cell Death Discovery*. 2022;8(1):18. doi:10.1038/s41420-021-00785-6
37. Kronstadt SM, Pottash AE, Levy D, Wang S, Chao W, Jay SM. Therapeutic potential of extracellular vesicles for sepsis treatment. *Adv Ther*. 2021;4(7). doi:10.1002/adtp.202000259
38. Huang W, Wang B, Ou Q, et al. ASC-expressing pyroptotic extracellular vesicles alleviate sepsis by protecting B Cells. *Mol Ther*. 2024;32(2):395–410. doi:10.1016/j.ymthe.2023.12.008
39. Wang J, Ma X, Si X, Han W. Sweroside functionalized with Mesenchymal Stem cells derived exosomes attenuates sepsis-induced myocardial injury by modulating oxidative stress and apoptosis in rats. *J Biomaterials Appl*. 2023;38(3):381–391. doi:10.1177/08853282231194317

40. Zhou Q, Xie M, Zhu J, et al. PINK1 contained in huMSC-derived exosomes prevents cardiomyocyte mitochondrial calcium overload in sepsis via recovery of mitochondrial Ca(2+) efflux. *Stem Cell Res Ther*. 2021;12(1):269. doi:10.1186/s13287-021-02325-6
41. Cao S, Huang Y, Dai Z, et al. Circular RNA mmu_circ_0001295 from hypoxia pretreated adipose-derived mesenchymal stem cells (ADSCs) exosomes improves outcomes and inhibits sepsis-induced renal injury in a mouse model of sepsis. *Bioengineered*. 2022;13(3):6323–6331. doi:10.1080/21655979.2022.2044720
42. Cheng X, Wang S, Li Z, He D, Wu J, Ding W. IL-1β-pretreated bone mesenchymal stem cell-derived exosomes alleviate septic endoplasmic reticulum stress via regulating SIRT1/ERK pathway. *Heliyon*. 2023;9(10):e20124. doi:10.1016/j.heliyon.2023.e20124
43. Liu J, Tang M, Li Q, Li Q, Dai Y, Zhou H. ATG2B upregulated in LPS-stimulated BMSCs-derived exosomes attenuates septic liver injury by inhibiting macrophage STING signaling. *Int Immunopharmacol*. 2023;117:109931. doi:10.1016/j.intimp.2023.109931
44. Zhang H, Zhao C, Jiang G, et al. Apelin rejuvenates aged human mesenchymal stem cells by regulating autophagy and improves cardiac protection after infarction. *Front Cell Develop Biol*. 2021;9:628463. doi:10.3389/fcell.2021.628463
45. Zhang H, Wan X, Tian J, et al. The therapeutic efficacy and clinical translation of mesenchymal stem cell-derived exosomes in cardiovascular diseases. *Biomed Pharmacotherapie*. 2023;167:115551. doi:10.1016/j.biopha.2023.115551
46. Fang J, Zhang Y, Chen D, Zheng Y, Jiang J. Exosomes and exosomal cargos: a promising world for ventricular remodeling following myocardial infarction. *Int j Nanomed*. 2022;17:4699–4719. doi:10.2147/IJN.S377479
47. Sun SJ, Wei R, Li F, Liao SY, Tse HF. Mesenchymal stromal cell-derived exosomes in cardiac regeneration and repair. *Stem Cell Rep*. 2021;16 (7):1662–1673. doi:10.1016/j.stemcr.2021.05.003
48. Pei Y, Xie S, Li J, Jia B. Bone marrow-mesenchymal stem cell-derived exosomal microRNA-141 targets PTEN and activates β-catenin to alleviate myocardial injury in septic mice. *Immuno and Immunotoxicology*. 2021;43(5):584–593. doi:10.1080/08923973.2021.1955920
49. Wang J, Zhang S, Li X, Gong M. LncRNA SNHG7 promotes cardiac remodeling by upregulating ROCK1 via sponging miR-34-5p. *Aging*. 2020;12(11):10441–10456. doi:10.18632/aging.103269
50. Xiong Y, Yang J, Tong H, Zhu C, Pang Y. HMGB1 augments cognitive impairment in sepsis-associated encephalopathy by binding to MD-2 and promoting NLRP3-induced neuroinflammation. *Psychogeriatrics*. 2022;22(2):167–179. doi:10.1111/psyg.12794
51. Chen G, Hou Y, Li X, Pan R, Zhao D. Sepsis-induced acute lung injury in young rats is relieved by calycosin through inactivating the HMGB1/MyD88/NF-κB pathway and NLRP3 inflammasome. *Int Immunopharmacol*. 2021;96:107623. doi:10.1016/j.intimp.2021.107623
52. Wang G, Jin S, Huang W, et al. LPS-induced macrophage HMGB1-loaded extracellular vesicles trigger hepatocyte pyroptosis by activating the NLRP3 inflammasome. *Cell Death Discovery*. 2021;7(1):337. doi:10.1038/s41420-021-00729-0
53. Meng X, Guo S, Zhang X, et al. HMGB1 inhibition reduces TDI-induced occupational asthma through ROS/AMPK/autophagy pathway. *Ecotoxicol Environ Saf*. 2023;266:115575. doi:10.1016/j.ecoenv.2023.115575